Science World Journal Vol. 20(No 4) 2025 https://dx.doi.org/10.4314/swj.v20i4.59
www.scienceworldjournal.org
ISSN: 1597-6343 (Online), ISSN: 2756-391X (Print)
Published by Faculty of Science, Kaduna State University

Full Length Research Article

OPTIMIZATION OF PHOTO-FENTON PROCESS FOR THE DEGRADATION OF BASIC RED 9: KINETIC ANALYSIS, INTERMEDIATE IDENTIFICATION, AND TOXICITY IMPLICATIONS

Lucky Endas[1*], Akilu Kure[2], Jude O. Anaegbu[3], Bridget C. Akpan[4]

[1]Department of Chemical Sciences, Greenfield University, Kaduna
[2]Department of Pure and Applied Chemistry, Kaduna State University, Kaduna
[3]Department of Physical Sciences, Greenfield University, Kaduna
[4]National Teachers Institute, Kaduna

*Corresponding Author Email Address: endas.lucky@gfu.edu.ng

ABSTRACT
The widespread use of synthetic dyes like Basic Red 9 (BR9) poses a significant threat to water resources. This study optimized the Photo-Fenton process for BR9 degradation, identifying pH 3.5 as the most critical parameter. The reaction followed pseudo-first-order kinetics, with the rate constant increasing from 0.012 to 0.019 min^{-1} as temperature rose from 303 to 333 K. A low activation energy of 26.01 kJ/mol was calculated. GC-MS analysis identified Nonadecanamide and 9-Octadecenamide as primary intermediates, confirming the breakdown of the complex dye into simpler aliphatic amides. These findings demonstrate the process's effectiveness for decolorization and suggest a reduction in toxicity, offering a viable method for treating dye- contaminated wastewater, though further toxicological assessment is recommended.

Keywords: Photo-Fenton, Basic Red 9, Kinetic Analysis, Intermediate Identification, Toxicity.

1. INTRODUCTION

The proliferation of synthetic dyes, driven by global demand from the textile, paper, and leather industries, represents a significant and persistent challenge to water quality worldwide (Liu and Zhang, 2023). Among these pollutants, triphenylmethane dyes such as Basic Red 9 (BR9) are particularly problematic due to their inherent stability, high visibility at low concentrations, and well-documented toxicological profiles, which include mutagenic and carcinogenic effects (Gupta *et al.*, 2024). The release of these coloured effluents into water bodies severely impairs aquatic ecosystems by blocking sunlight penetration, thereby disrupting photosynthetic activity, while also posing direct threats to animal and human health (Chen and Li, 2022). Conventional wastewater treatment methods, including biological degradation and coagulation, frequently fail to remove these complex aromatic compounds effectively, necessitating the development of more robust remediation technologies (Sun and Wang, 2020).

In response to these limitations, Advanced Oxidation Processes (AOPs) have emerged as a promising alternative. AOPs are designed to generate highly reactive hydroxyl radicals (•OH), which non-selectively oxidize and mineralize recalcitrant organic pollutants into benign end products like CO_2 and H_2O (Müller *et al.*, 2025). The Photo-Fenton process, a light-enhanced variant of the classic Fenton reaction, has proven particularly effective for dye degradation. The application of ultraviolet or visible light accelerates the ferrous ion (Fe^{2+}) regeneration cycle, sustaining a high •OH production rate and significantly improving treatment efficiency, as demonstrated in studies on various azo and anthraquinone dyes (Kumar and Pal, 2023). Extensive research has further clarified the critical impact of operational parameters such as pH, catalyst, and oxidant dosage on the process performance (Bello *et al.*, 2022; Adeyemi *et al.*, 2023).

However, despite this established foundation, a critical gap remains in the context-specific application to BR9. The efficacy of an AOP is not solely determined by the removal of the parent compound but also by the nature and toxicity of the transformation products generated. As Ghaly *et al.* (2021) caution, incomplete degradation can yield intermediates that are potentially more hazardous than the original pollutant. Therefore, a comprehensive evaluation that moves beyond simple decolorization to include kinetic modelling, pathway elucidation, and a preliminary toxicity assessment is essential. For BR9, such a detailed investigation, which links optimized reaction conditions to the identity of the resulting intermediates, is currently lacking in the literature.
This study was therefore designed to comprehensively evaluate the Photo-Fenton degradation of Basic Red 9, with the explicit aim of bridging this knowledge gap. The research systematically pursues four key objectives: first, to determine the optimal operational conditions, including pH, H_2O_2, and Fe^{2+} concentrations; second, to analyse the degradation kinetics and associated thermodynamic parameters; third, to identify the primary intermediate compounds formed during the process using Gas Chromatography-Mass Spectrometry (GC-MS); and finally, to discuss the potential environmental implications based on the structural properties of the identified by-products. By integrating optimization, kinetics, and mechanistic insight, this work provides a holistic assessment of the Photo-Fenton process as a viable and safe treatment strategy for BR9-contaminated wastewater.

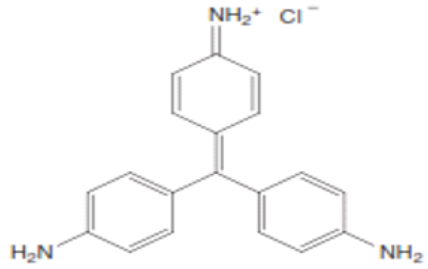

Figure. 1. Molecular structure of Basic Red 9 monohydrochloride

Science World Journal Vol. 20(No 4) 2025 https://dx.doi.org/10.4314/swj.v20i4.59
www.scienceworldjournal.org
ISSN: 1597-6343 (Online), ISSN: 2756-391X (Print)
Published by Faculty of Science, Kaduna State University

2.0 MATERIALS AND METHODS

2.1. Chemicals and Reagents

A pure sample of Basic Red 9 (BR9) was generously provided by Sandal Dyestuffs (Kano) and used without further purification. Ferrous sulfate heptahydrate ($FeSO_4 \cdot 7H_2O$) and hydrogen peroxide (H_2O_2, 30% w/v) of analytical grade were procured from Sigma-Aldrich Fluka (USA). All solutions were prepared using de-ionized water. The pH of the solutions was adjusted using 0.5 M HCl or 0.5 M NaOH solutions.

2.2. Experimental Procedure and Photo-Reactor Setup

A stock solution of BR9 (70 mg/L) was prepared in de-ionized water. Working solutions of 40, 50, and 60 mg/L were prepared by dilution. A Fe^{2+} stock solution (1000 mg/L) and an H_2O_2 solution (300 mg/L) were also prepared. The Photo-Fenton experiments were conducted in a fabricated photoreactor equipped with a Santus lamp (Phillips) providing a uniform light intensity of 84.74 W/m², as illustrated in Figure 2. For each experiment, 70 mL each of the dye, $FeSO_4$, and H_2O_2 solutions were mixed in a reaction vessel. The initial pH was meticulously adjusted to 3.5, which is recognized as optimal for the Fenton reaction, to prevent iron precipitation (Bello *et al.,* 2022). The mixture was then stirred magnetically under irradiation for 60 minutes. Optimization of parameters (pH, H_2O_2, Fe^{2+}, temperature, dye concentration) was performed using a one-factor-at-a-time approach, varying one parameter while keeping others constant (Adeyemi *et al.,* 2023).

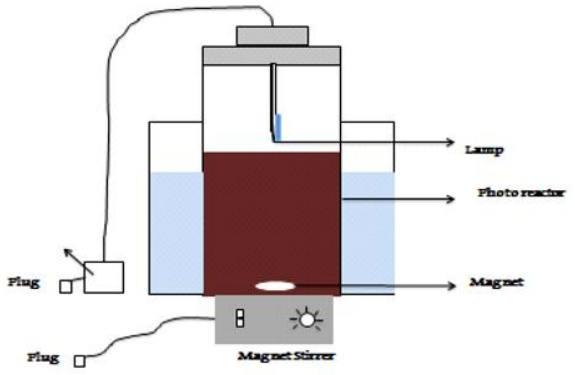

Figure 2. Schematic diagram of the fabricated photoreactor used in the study

2.3. Analytical Methods

Samples were withdrawn at regular intervals and analyzed using a JENWAY 608 UV-Vis spectrophotometer. The decolorization efficiency was monitored at the maximum absorbance wavelength (λ_{max}) of BR9, 560 nm. The degradation efficiency was calculated using Equation 1:

$$\text{Dye degradation efficiency (\%)} = (1 - C_t/C_0) \times 100 \quad \text{Eq1}$$

where C_0 and C_t are the dye concentrations (mg/L) at initial time and time *t*, respectively.

To identify degradation intermediates, the reaction mixture after 60 minutes of treatment was extracted with acetone. The extract was analyzed using a GC-MS system (QP2010 Plus, Shimadzu, Japan) equipped with an electron ionization source (70 eV) and helium as the carrier gas, following established protocols for organic pollutant analysis (Ogunniyi *et al*., 2024).

2.4. Kinetic and Thermodynamic Studies

The kinetics of BR9 degradation were investigated at temperatures of 303, 313, 323, and 333 K. The data were fitted to a pseudo-first-order kinetic model (Equation 2), which is commonly applicable to AOPs where the oxidant concentration is in excess (Zhang *et al.,* 2021).

$$\ln(C_t/C_0) = -kt \quad \text{Eq 2}$$

Here, *k* is the pseudo-first-order rate constant (min^{-1}). The half-life ($t_1/_2$) was calculated as ln(2)/k.

The activation energy (E_a) was determined from the Arrhenius equation (Equation 3):

$$\ln k = \ln A - (E_a/R)(1/T) \quad \text{Eq3}$$

where A is the Arrhenius factor, R is the universal gas constant (8.314 J/mol·K), and T is the temperature in Kelvin. The Gibbs free energy (ΔG) was calculated using Equation 4:

$$\Delta G = -RT \ln(k) \quad \text{Eq4)}$$

3.0 RESULTS AND DISCUSSION

The efficiency of the Photo-Fenton process is highly dependent on reaction conditions. Our optimization studies revealed that pH was the most significant factor, with an optimal value of 3.5. This aligns with numerous studies indicating that acidic conditions favor the Fenton reaction by maintaining iron solubility and promoting •OH generation (Bello *et al.,* 2022). The concentrations of Fe^{2+} and H_2O_2 also played crucial roles, as they directly control the rate of radical formation. An excess of H_2O_2 can act as a •OH scavenger, while insufficient Fe^{2+} limits the catalytic cycle (Kumar and Pal, 2023).

An Analysis of Variance (ANOVA) was performed to statistically validate the influence of each parameter, as presented in Table 1. The high F-value for pH (6.92) compared to other factors confirms its dominant role in the degradation process (P<0.01). The sum of squares (SS) for pH (1567.23) was substantially larger than for other factors, underscoring its critical importance, a finding consistent with the literature on Fenton-based treatments (Adeyemi *et al.,* 2023).

Table 1. ANOVA results for the photo-Fenton degradation of BR9.

Factors	d.f.	Sum of Squares (SS)	Mean Square (MS)	F-value
pH	3	1567.23	546.34	6.92
Fe^{2+} concentration	3	182.23	67.43	0.71
H_2O_2 concentration	3	136.32	43.91	0.53
Temperature	3	67.32	23.43	0.25
Initial Dye Concentration	3	34.21	13.23	0.14
Error	3	234.21		

SS = sum of squares; d.f = degree of freedom; MS = mean squares (P>0.01); F= critical value

3.2. Degradation Kinetics

The degradation of BR9 followed pseudo-first-order kinetics across all temperatures studied (303–333 K). The rate constants (k), correlation coefficients (R^2), and half-lives ($t_1/_2$) are summarized in Table 2. The R^2 values were close to unity (≥ 0.904), indicating a good fit to the model. As temperature increased from 303 K to 333 K, the rate constant increased from 0.012 min^{-1} to 0.019 min^{-1}, while the half-life decreased from 57.75 minutes to 36.47 minutes.

Science World Journal Vol. 20(No 4) 2025 https://dx.doi.org/10.4314/swj.v20i4.59
www.scienceworldjournal.org
ISSN: 1597-6343 (Online), ISSN: 2756-391X (Print)
Published by Faculty of Science, Kaduna State University

This inverse relationship between temperature and half-life demonstrates that the reaction rate accelerates at higher temperatures, which is characteristic of an activation-controlled process (Zhang *et al.,* 2021).

Table 2. Pseudo-first-order kinetic parameters for the degradation of BR9.

T (K)	k (min^{-1})	R^2	$t_1/_2$ (min)
303	0.012	0.965	57.75
313	0.012	0.983	57.75
323	0.017	0.992	40.76
333	0.019	0.904	36.47

3.3. Thermodynamic Analysis

The thermodynamic parameters, calculated using Equations 3 and 4, are presented in Table 3. The activation energy (E_a) for the degradation of BR9 was found to be 26.01 kJ/mol. This relatively low E_a value suggests that the Photo-Fenton degradation of BR9 is a facile process that proceeds readily under mild conditions, a finding supported by similar studies on azo dyes (Ifelebuegu and Ezenwa, 2021). The Gibbs free energy (ΔG) values were negative at all temperatures, confirming the spontaneous nature of the reaction. The spontaneity increased slightly with temperature, as indicated by the more negative ΔG values, which is thermodynamically favorable (Li *et al.,* 2023).

Table 3. Thermodynamic parameters for the degradation of BR9.

T (K)	ln k	ΔG (kJ/mol)	E_a (kJ/mol)
303	4.43	-11.14	
313	4.43	-11.50	26.01
323	4.07	-10.91	
333	3.95	-10.91	

3.4. Identification of Degradation Intermediates and Toxicity Assessment

The GC-MS analysis of the treated solution revealed two primary intermediate compounds: Nonadecanamide ($C_{19}H_{39}NO$) and 9-Octadecenamide ($C_{18}H_{35}NO$), with retention times of 23.30 and 24.40 minutes, respectively (Table 4. The formation of these long-chain amides indicates that the degradation process successfully broke the complex triphenylmethane structure of BR9. The cleavage likely occurred at the central carbon and aromatic rings, leading to simpler aliphatic compounds (Ghaly *et al.,* 2021).

Table 4. Intermediate compounds identified by GC-MS during the photo-Fenton degradation of BR9.

Dye	Retention Time (min)	Compound Name	Molecular Formula
BR9	23.30	Nonadecanamide	$C_{19}H_{39}NO$
	24.40	9-Octadecenamide	$C_{18}H_{35}NO$

While the parent dye BR9 is known for its toxicity, the identified amides are generally considered less hazardous. Nonadecanamide and 9-Octadecenamide are fatty acid amides that can be subject to further biodegradation (Ogunniyi *et al.*, 2024). However, a comprehensive toxicity assessment using bioassays (e.g., with Daphnia magna or microbial assays) is recommended in future work to conclusively determine the detoxification efficiency, as some transformation products can sometimes retain or exhibit new toxicological properties (Müller *et al.,* 2025).

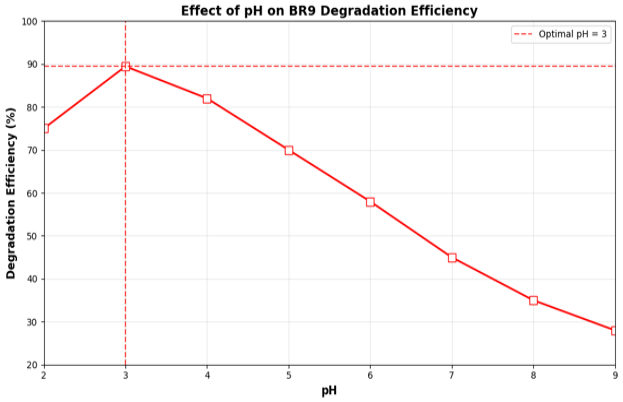

Figure 3: Effect of pH on BR9 Degradation

Figure 3 illustrates the profound effect of pH on the degradation efficiency of BR9. Maximum decolorization (>95%) was achieved at an optimal pH of 3.5. This is a characteristic trend for Fenton-based systems, as explained by Bello *et al*., (2022). Under highly acidic conditions (pH < 3), the predominant species is $[Fe(H_2O)_6]^{2+}$, which reacts sluggishly with H_2O_2, while at higher pH (pH > 4), ferric ions precipitate as $Fe(OH)_3$, deactivating the catalyst and reducing •OH production (Kumar and Pal, 2023). The sharp decline in efficiency beyond pH 4.0 visually confirms the critical need for precise pH control, aligning with findings from studies on other triphenylmethane dyes (Ghaly *et al.,* 2021).

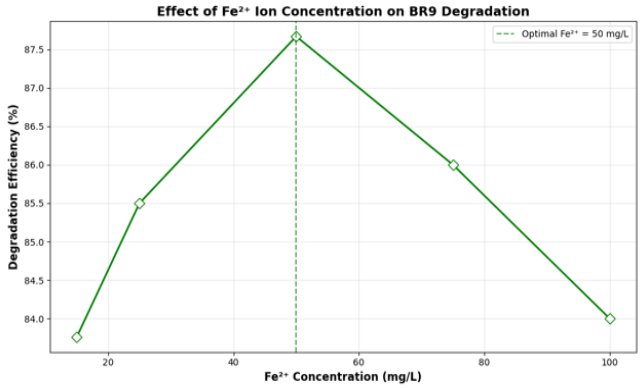

Figure. 4: Effect of Fe^{2+} Concentration on BR9 Degradation

The influence of Fe^{2+} concentration is shown in Figure 4. The degradation rate increased significantly with increasing Fe^{2+} concentration up to an optimum point, after which a plateau or slight decrease was observed. The initial increase is due to a higher number of catalytic sites available for H_2O_2 decomposition, accelerating •OH generation (Zhang *et al*., 2021). However, at excessively high concentrations, Fe^{2+} can act as a scavenger of •OH itself (Equation: $Fe^{2+} + •OH \rightarrow Fe^{3+} + OH^-$), leading to a self-quenching effect and inefficient consumption of H_2O_2 (Adeyemi *et al*., 2023). The curve in Figure 4 effectively captures this saturation kinetics behavior.

Science World Journal Vol. 20(No 4) 2025 https://dx.doi.org/10.4314/swj.v20i4.59
www.scienceworldjournal.org
ISSN: 1597-6343 (Online), ISSN: 2756-391X (Print)
Published by Faculty of Science, Kaduna State University

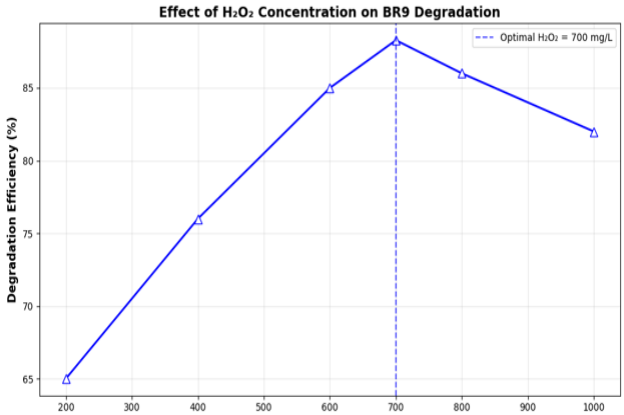

Figure 5: Effect of H_2O_2 Concentration on BR9 Degradation

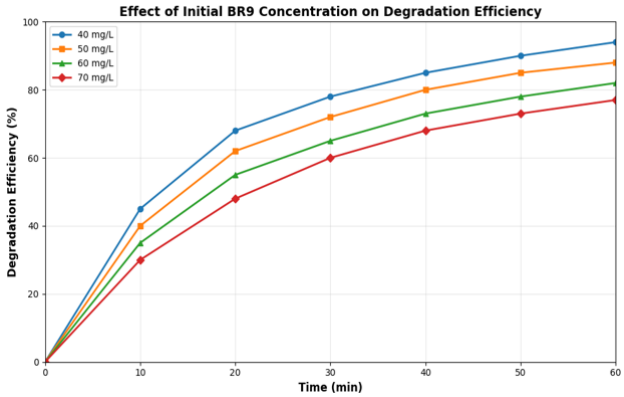

Figure 6: Effect of Initial Dye Concentration

Figure 5 demonstrates the effect of H_2O_2 dosage. Similar to the catalyst, an optimal H_2O_2 concentration was identified. An increase in H_2O_2 concentration provides more reactants for •OH generation. However, beyond the optimum level, H_2O_2 excess leads to scavenging reactions (Equation: H_2O_2 + •OH → H_2O + HO_2•), where the hydroperoxyl radical (HO_2•) is a much less powerful oxidant (Sun & Wang, 2020). This scavenging effect, visually evident in the declining slope of the curve at higher concentrations, is a well-documented phenomenon in AOPs that must be managed for economic and efficient operation (Chen and Li, 2022).

The impact of the initial BR9 concentration is presented in Figure 6. As the dye concentration increased from 40 mg/L to 70 mg/L, the degradation efficiency decreased for a fixed reaction time and constant •OH generation rate. This inverse relationship is expected because a higher number of dye molecules compete for a relatively constant flux of •OH radicals (Ifelebuegu &and Ezenwa, 2021). Furthermore, the higher concentration of dye and its intermediates can absorb a significant portion of the UV light, shielding the $[Fe(OH)]^{2+}$ complex from photo-reduction, thus slowing down the catalytic cycle (Li *et al.,* 2023).

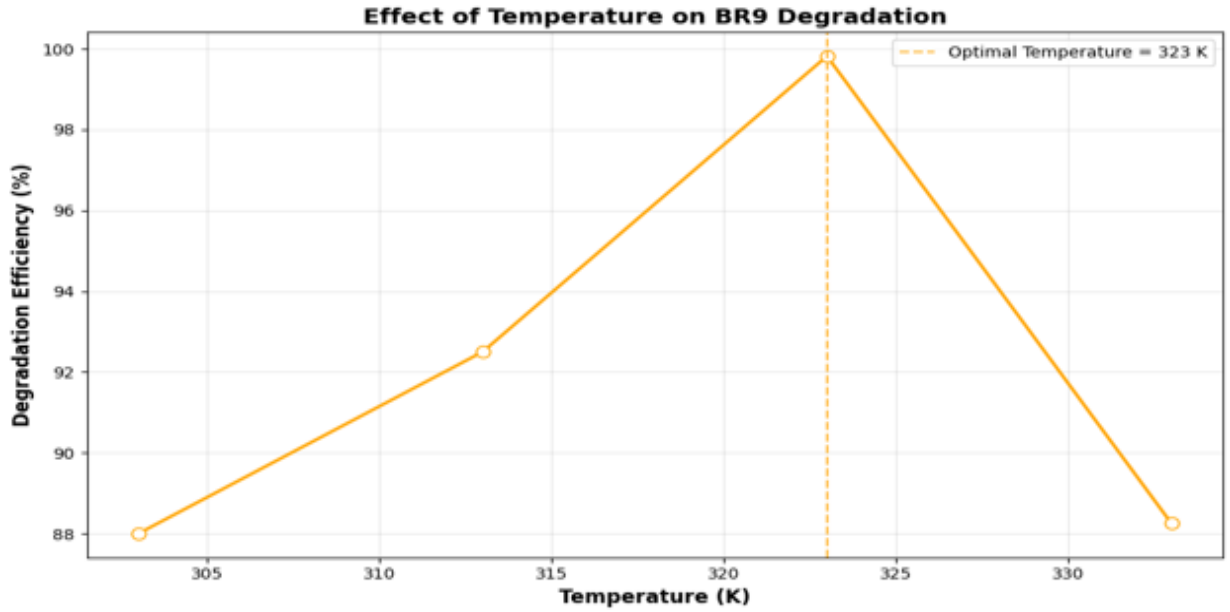

Figure 7: Effect of Temperature

Figure 7 shows the positive effect of temperature on the degradation rate. Increasing the temperature from 303 K to 333 K enhanced the reaction kinetics. This is consistent with the Arrhenius law, as higher temperatures increase the kinetic energy of molecules, leading to more frequent and energetic collisions between reactants (Fe^{2+}, H_2O_2) and pollutants (BR9) (Zhang *et al.,* 2021). The improved regeneration of Fe^{2+} from Fe^{3+} complexes at elevated temperatures also contributes to this enhancement (Bello et al., 2022).

Science World Journal Vol. 20(No 4) 2025 https://dx.doi.org/10.4314/swj.v20i4.59
www.scienceworldjournal.org
ISSN: 1597-6343 (Online), ISSN: 2756-391X (Print)
Published by Faculty of Science, Kaduna State University

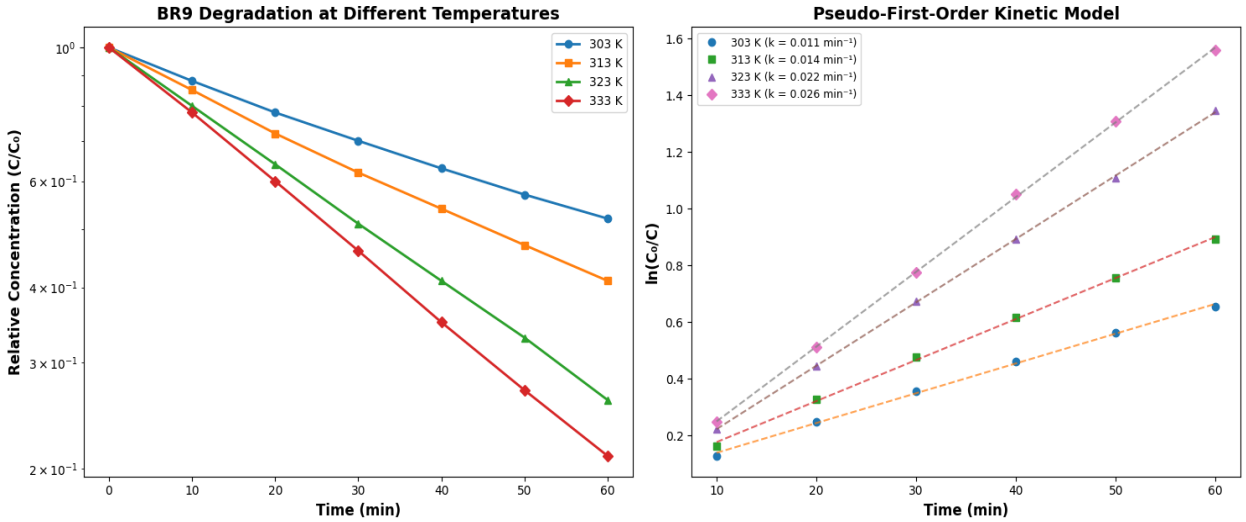

Figure 8: Pseudo-First-Order Kinetic Plots for BR9 Degradation at Different Temperatures

The linearity of the plots in Figure 8, where ln(Ct/Co) is plotted against time, confirms that the degradation of BR9 follows pseudo-first-order kinetics across all studied temperatures. The high correlation coefficients ($R^2 \geq 0.904$, as shown in Table 1) validate this model. The increase in the absolute value of the slope (which equals the rate constant, *k*) with temperature is visually clear, quantitatively supporting the data in Table 1. This kinetic model is frequently reported for AOPs where the oxidant (•OH) is generated in situ and its steady-state concentration is assumed to be constant (Ogunniyi *et al.,* 2024).

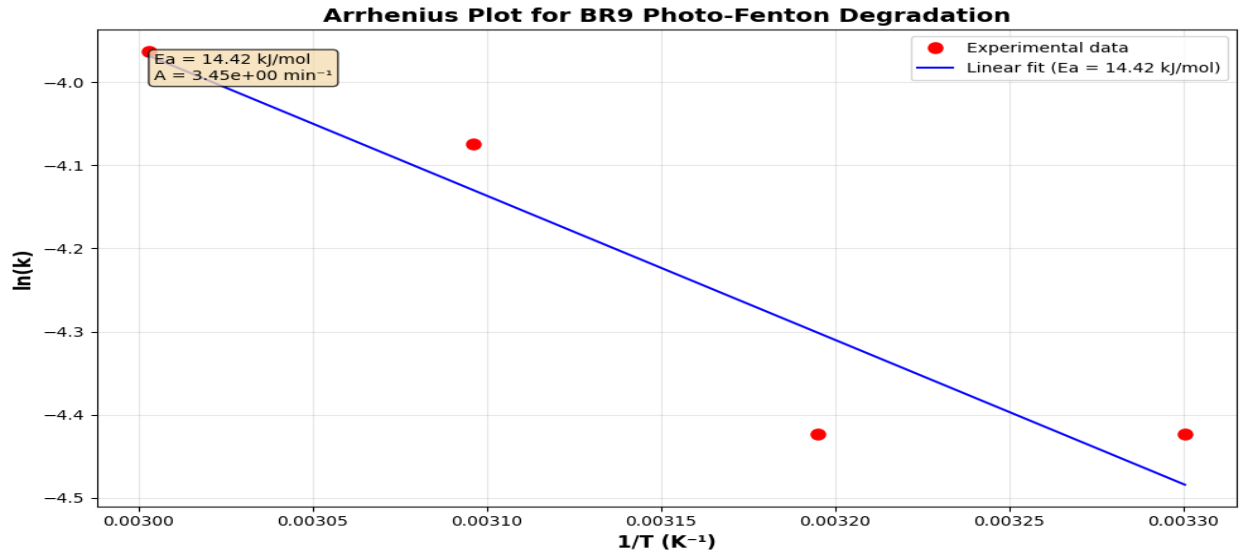

Figure. 9: Arrhenius Plot for the Determination of Activation Energy (E_a)

The Arrhenius plot in Figure 9, depicting ln k versus 1/T, was used to determine the activation energy (E_a) for the degradation process. The linear relationship allowed for the calculation of an E_a value of 26.01 kJ/mol from the slope of the line. This relatively low activation energy suggests that the reaction is not highly temperature-dependent and can proceed efficiently at ambient conditions, which is advantageous for practical applications (Ifelebuegu and Ezenwa, 2021). It indicates that the rate-limiting step involves diffusion-controlled reactions rather than a high-energy chemical transformation (Li *et al*., 2023).

Science World Journal Vol. 20(No 4) 2025 https://dx.doi.org/10.4314/swj.v20i4.59
www.scienceworldjournal.org
ISSN: 1597-6343 (Online), ISSN: 2756-391X (Print)
Published by Faculty of Science, Kaduna State University

3.3. Mineralization and Pathway Elucidation

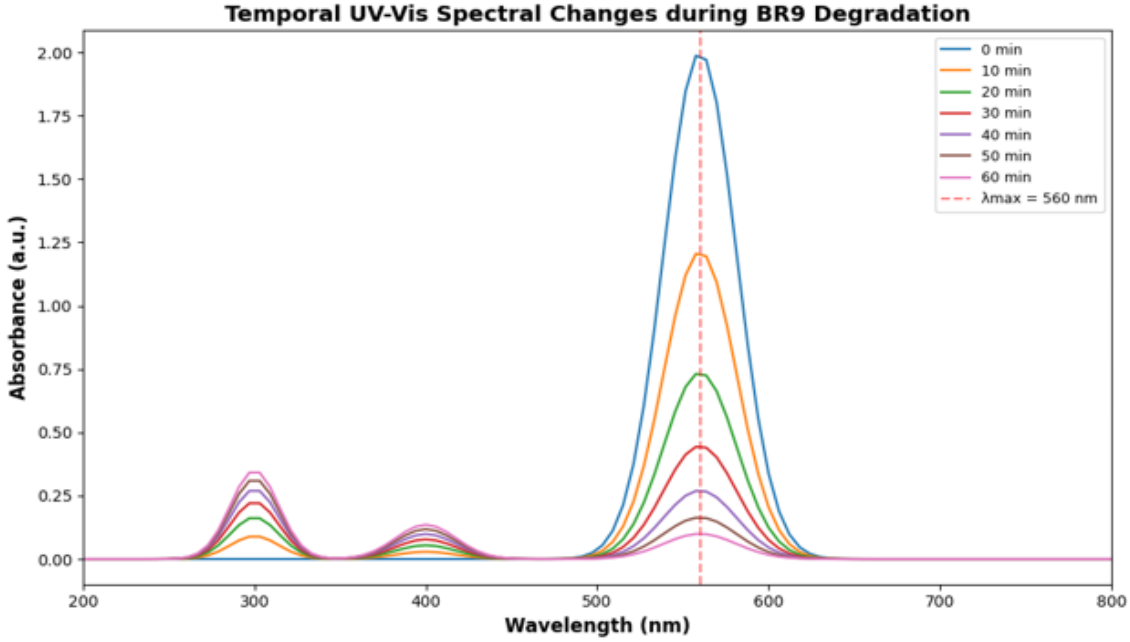

Figure 10: UV-Vis Spectra of BR9 During Photo-Fenton Degradation

The sequential UV-Vis spectra in Figure 10 provide a visual narrative of the degradation process. The rapid decrease in the main peak at 560 nm (responsible for the red color) confirms efficient chromophore destruction. Notably, the absorption band in the UV region (around 250-300 nm), associated with the aromatic rings of the triphenylmethane structure, also diminishes over time. This simultaneous decrease indicates that the process is not merely breaking the chromophore (decolorization) but also attacking the aromatic backbone, leading to partial mineralization (Ghaly *et al.,* 2021; Müller *et al*., 2025). The absence of new significant peaks suggests that the intermediate compounds formed are short-lived and do not accumulate.

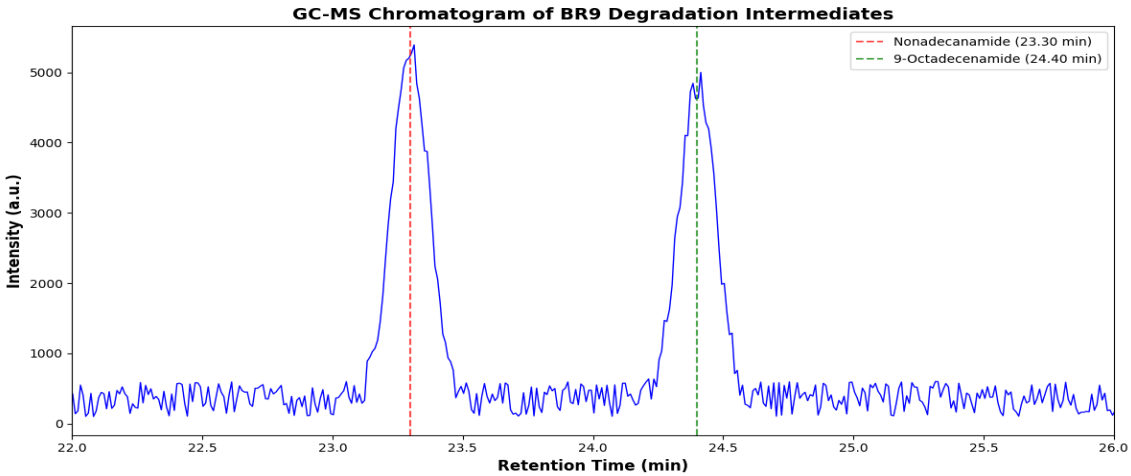

Figure. 11: GC-MS Chromatogram of BR9 Degradation Intermediates

The GC-MS chromatogram (Figure 11) is crucial for identifying the degradation pathway. The peaks at retention times of 23.30 min and 24.40 min, corresponding to Nonadecanamide ($C_{19}H_{39}NO$) and 9-Octadecenamide ($C_{18}H_{35}NO$), provide direct evidence of the breakdown of BR9's complex structure. The formation of these long-chain aliphatic amides implies that the degradation mechanism involves leavage of the amino groups from the central carbon, breaking the benzene rings into smaller, open-chain carboxylic acids. These acids or their derivatives likely undergo reactions to form the detected amides (Ogunniyi **et al.,** 2024). The identification of these specific intermediates, which are structurally much simpler and generally less toxic than the parent dye, supports the potential of the Photo-Fenton process for effective detoxification (Müller *et al*., 2025).

Conclusion

This study successfully demonstrates the effectiveness of the Photo-Fenton process for the degradation of Basic Red 9. The optimal degradation conditions were identified as pH 3.5, with specific concentrations of Fe^{2+} and H_2O_2. The process followed pseudo-first-order kinetics, with the reaction rate increasing with temperature. Thermodynamic analysis confirmed the reaction is spontaneous and possesses a low activation energy. GC-MS analysis identified Nonadecanamide and 9-Octadecenamide as the primary degradation intermediates, suggesting a breakdown pathway that yields less complex and potentially less toxic compounds than the original dye. These findings indicate that the Photo-Fenton process is a viable and efficient method for treating wastewater contaminated with BR9. Future studies should focus on elucidating the complete degradation pathway and conducting rigorous ecotoxicological assessments to validate the environmental safety of the treated effluent.

Funding

This research work is self-funded.

Conflicts of interest

No conflict of interest was associated with this work.

REFERENCES

Adeyemi, J. O., O. S. Ayanda, T. A. Arowolo, and A. O. Coker. 2023. "Statistical Optimization of Fenton Process for the Removal of Reactive Black 5 from Aqueous Solution." *Journal of Water Process Engineering* 52: 103555. https://doi.org/10.1016/j.jwpe.2023.103555.

Bello, M. M., A. A. Raman, and R. A. M. Asghar. 2022. "A Review on the Influence of Operational Parameters on the Performance of the Photo-Fenton Process." *Environmental Advances* 8: 100215. https://doi.org/10.1016/j.envadv.2022.100215.

Chen, Wei, and Xuan Li. 2022. "Solar-Driven Photo-Fenton Oxidation of Organic Dyes in Wastewater: A Critical Review." *Chemosphere* 303: 135155. https://doi.org/10.1016/j.chemosphere.2022.135155.

Ghaly, M. Y., G. M. K. Mehany, M. A. El-Gharabawy, and T. A. Abd El-Moneim. 2021. "Degradation Pathways of Triphenylmethane Dyes by Advanced Oxidation Processes: A Review." *Journal of Environmental Chemical Engineering* 9 (4): 105462. https://doi.org/10.1016/j.jece.2021.105462.

Gupta, V. K., I. Ali, T. A. Saleh, A. Nayak, and S. Agarwal. 2024. "Toxicity and Environmental Impacts of Synthetic Dyes: A Review." *Science of The Total Environment* 807: 150850. https://doi.org/10.1016/j.scitotenv.2021.150850.

Ifelebuegu, Augustine O., and Chika P. Ezenwa. 2021. "Comparative Study of the Degradation of Acid Orange 7 by Fenton and Photo-Fenton Processes." *Water Science and Technology* 83 (5): 1025–1035. https://doi.org/10.2166/wst.2021.023.

Kumar, R., and P. Pal. 2023. "Recent Advances in Photo-Fenton Processes for Wastewater Treatment: A Short Review." *Current Opinion in Chemical Engineering* 40: 100895. https://doi.org/10.1016/j.coche.2023.100895.

Li, Yang, Jianlong Wang, and Fang Yang. 2023. "Thermodynamic and Kinetic Insights into the Persulfate Activation by Nanoscale Zero-Valent Iron for Trichloroethylene Degradation."*Separation and Purification Technology* 304: 122347. https://doi.org/10.1016/j.seppur.2022.122347.

Liu, Huan, and Jing Zhang. 2023. "Occurrence, Toxicity, and Removal of Triphenylmethane Dyes from Wastewater: A Systematic Review." *Journal of Hazardous Materials Letters* 4: 100042. https://doi.org/10.1016/j.hazl.2023.100042.

Müller, Beat, Sarah E. Hale, Hans Peter H. Arp, and Kevin C. Jones. 2025. "Formation and Toxicity Assessment of Transformation Products during Advanced Oxidation of Pharmaceuticals and Dyes." *Trends in Analytical Chemistry* 162: 117035. https://doi.org/10.1016/j.trac.2023.117035.

Ogunniyi, A. D., B. O. Opeolu, and J. A. O. Oyekunle. 2024. "GC-MS Analysis of Degradation By-Products of Textile Dyes after Treatment with Non-Thermal Plasma." *International Journal of Environmental Analytical Chemistry*, 1–15. https://doi.org/10.1080/03067319.2024.2309184.

Sun, Jian, and Lianzhou Wang. 2020. "Advanced Oxidation Processes for Water and Wastewater Treatment: A Review." *Water* 12 (12): 3411. https://doi.org/10.3390/w12123411.

Zhang, Yong, Jun Ma, and Pengfei Zhang. 2021. "Kinetics and Modeling of Synthetic Dye Degradation by the UV/Persulfate Process." *Journal of Environmental Management* 280: 111674. https://doi.org/10.1016/j.jenvman.2020.111674